Acta Crystallographica Section F
Structural Biology and Crystallization Communications
ISSN 1744-3091

Crystallization and initial X-ray data of abscisic acid receptor PYL3 in the presence of (−)-ABA

Xingliang Zhang,[a]* Qi Zhang[b] and Guoqiang Wang[b]

[a]Clinical Medicine Research Center, Affiliated Hospital of Guangdong Medical College, Zhanjiang, Guangdong 524001, People's Republic of China, and [b]State Key Laboratory of Agrobiotechnology, College of Biological Sciences, China Agricultural University, Beijing 100193, People's Republic of China

Correspondence e-mail: cheungxingliang@gmail.com

Received 18 December 2012
Accepted 23 March 2013

Abscisic acid (ABA) modulates many complicated developmental processes and responses to environmental stimuli. Recently, several (+)-ABA signalling mechanisms by the RCAR/PYR1/PYL family of proteins (PYLs) have been proposed. However, the mechanism of the recognition and binding of the unnatural ligand (−)-ABA by PYLs has not yet been elucidated. In the present study, the expression, purification and crystallization of PYL3 in complex with (−)-ABA are reported. Diffraction data were refined to 2.65 Å resolution for this complex in space group $P6_5$. These findings will help to explain the stereospecificity of PYLs for (−)-ABA and to explore the selective ABA agonists.

1. Introduction

Abscisic acid (ABA) plays pivotal roles in the regulation of seed germination, bud dormancy, plant growth and stomatal aperture and in the response to abiotic stresses (Cutler *et al.*, 2010; Raghavendra *et al.*, 2010). The ABA response allows the plant to adapt to developmental and environmental conditions. Therefore, understanding the detailed ABA pathway is one of the most important goals in plant research.

The recent identification of the ABA receptor was an important milestone in ABA signalling. Firstly, the RCAR/PYR1/PYL family of proteins (hereafter referred to as PYLs) were identified to be ABA receptors by genetic and biochemical studies (Ma *et al.*, 2009; Park *et al.*, 2009; Santiago, Rodrigues *et al.*, 2009). The crystal structures of PYR1 and PYL1–2 were then determined by several research groups (Melcher *et al.*, 2009; Miyazono *et al.*, 2009; Nishimura *et al.*, 2009; Santiago, Dupeux *et al.*, 2009; Yin *et al.*, 2009). Subsequently, *in vitro* reconstitution of the ABA-dependent signalling pathway of ABA was confirmed (Fujii *et al.*, 2009). The ABA-independent inhibition of PP2Cs by a subclass of PYL proteins was another important discovery (Hao *et al.*, 2011). Two distinct classes of receptors, dimers and monomers, with different intrinsic affinities for ABA have been identified (Dupeux *et al.*, 2011). Pyrabactin was a selective ABA agonist/antagonist for identification of proteins from the PYL family (Park *et al.*, 2009). The structures of complexes of PYR1 and PYL1–2 with pyrabactin have been reported (Hao *et al.*, 2010; Melcher *et al.*, 2010; Peterson *et al.*, 2010; Yuan *et al.*, 2010). Recently, we reported a novel *trans*-homodimer intermediate PYL3 bound to (+)-ABA or pyrabactin (Zhang, Zhang *et al.*, 2012).

S-(+)-ABA exists naturally, with one asymmetric C atom at C1′ (Supplementary Fig. S1A[1]). Many plant research groups have focused on its physiological and genetic activities. Similarly, the biological activity and importance of the synthetic *R*-(−)-ABA (Supplementary Fig. S1B) have also been investigated (Milborrow, 1974; Cutler *et al.*, 2010). In many assays, such as stomatal closure, (−)-ABA showed weak activity. However, in other assays, for example seed germination (Nambara *et al.*, 2002) and plant-tissue growth (Milborrow, 1974), (−)-ABA has been found to have comparable activity to (+)-ABA. These results imply that there must be some receptors that recognize (−)-ABA. The inhibitory effect of

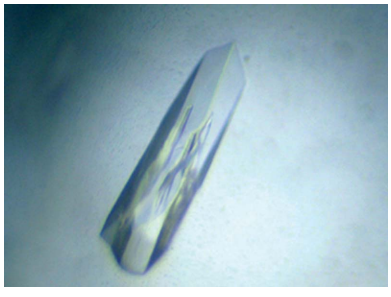

[1] Supplementary material has been deposited in the IUCr electronic archive (Reference: PU5393).

HAB1 activity by (−)-ABA was mediated by PYL5 and PYL8 (Ma *et al.*, 2009). In addition, PYL5 strongly binds to (−)-ABA, but PYL9 is insensitive to it (Ma *et al.*, 2009; Park *et al.*, 2009; Santiago, Rodrigues *et al.*, 2009). According to the PYR1–(+)-ABA structure, Nishimura and coworkers suggested that the (−)-ABA ring was flipped ∼180° from the (+)-ABA ring and that the ring-flipped binding of (−)-ABA provides a structural basis for its varying bioactivity (Nishimura *et al.*, 2009). Based on the binding mode of (+)-ABA-bound PYL2, Melcher and coworkers proposed that the dimethyl group that is flipped in the (−)-isomer would cause a steric collision between the dimethyl group and the narrow pocket that accommodates the monomethyl group (Melcher *et al.*, 2009). Thus, the arrangement of the hydrophobic residues that surround the cyclohexene moiety was proposed to underlie the stereoselectivity of the ABA isomers (Umezawa *et al.*, 2010). However, the orientation of (−)-ABA in the pocket of PYLs and the basis of the stereospecificity of PYLs for both ABA enantiomers remain unclear. Among the PYLs, we have focused on PYL3 and its interaction with ligands such as (+)-ABA, (−)-ABA and pyrabactin (Zhang, Zhang *et al.*, 2012; Zhang, Wu *et al.*, 2012). PYL3 showed productive binding to (+)-ABA and (−)-ABA, in contrast to pyrabactin. Here, the PYL3–(−)-ABA complex was successfully crystallized in space group $P6_5$ and X-ray data were collected to 2.65 Å resolution. These results will pave the way for illustrating the selection of ABA stereoisomers by PYLs.

2. Materials and methods

2.1. Protein expression

PYL3 (AT1G73000.1) and several fragments (residues 15–209, 21–209, 25–209 and 48–209) were engineered into prokaryotic fusion expression vectors as described elsewhere (Zhang, Wu *et al.*, 2012). Briefly, PYL3 or fragments with *Bam*HI/*Xho*I sites were inserted into pET28a or pGEX-4T-2, in which the thrombin site was replaced by a TEV site. The recombinant plasmids were transformed into *Escherichia coli* TOP10 competent cells. The inserted fragments of interest were verified by DNA sequencing. The positive recombinant plasmids were transformed into *E. coli* strain BL21 (DE3) cells (Novagen) for expression of target proteins.

BL21 (DE3) cells containing recombinant plasmid were incubated in 2.0 ml LB medium at 310 K overnight and then transferred to 1.0 l LB medium at 310 K supplemented with antibiotic at a final concentration of 50 µg ml^{-1}. When the absorbance at 600 nm of the cell culture reached ∼0.8, 0.2 m*M* isopropyl *β*-D-1-thiogalactopyranoside (IPTG) was added to induce expression of the target protein, which continued for 20 h at 293 K.

2.2. Protein purification

Cells were pelleted by centrifugation at 4000 rev min^{-1} at 277 K for 30 min. The pellet was then vortexed in 30 ml lysis buffer consisting of 20 m*M* Tris–HCl pH 8.0, 500 m*M* NaCl, 1 m*M* DTT, 10 m*M* PMSF. Cell disruption was carried out by sonication. The lysate was centrifuged at 20 000 rev min^{-1} for 20 min and the supernatant was filtered using a 0.45 µm filter membrane. The filtered supernatant was loaded onto a Glutathione Sepharose 4 Fast Flow resin column (GE Healthcare) and the flowthrough was passed through the column again. The resin column was washed with 20 column volumes of buffer I (20 m*M* Tris–HCl pH 8.0, 150 m*M* NaCl, 1 m*M* DTT). To remove the GST tag, a small amount of 6×His-tagged TEV protease was added to the Glutathione Sepharose 4 Fast Flow resin column on ice overnight. The digestion components were then passed through a Glutathione Sepharose 4 Fast Flow resin column to remove residual GST fusion proteins followed by a Profinity IMAC Ni-charged resin column (Bio-Rad) to remove TEV protease. The target protein free of the GST tag was further purified by gel filtration (Superdex 200 HR10/300 GL, GE Healthcare). The final concentration of PYL3 or fragment protein was about 20 mg ml^{-1} in buffer I. The protein concentration was measured by the Bradford method using Coomassie Brilliant Blue G-250 (595 nm).

To obtain homogeneous PYL3–(−)-ABA complex, (−)-ABA (Sigma) was dissolved in buffer I to give a stock solution of 100 m*M* and adjusted to pH 8.0 with NaOH solution. (−)-ABA was then incubated with the freshly purified PYL3 or fragment protein for 2 h at 277 K. The mixture was subjected to gel filtration to remove excess free (−)-ABA.

Table 1
Data-collection and processing statistics.

Values in parentheses are for the highest resolution shell.

Wavelength (Å)	1.0000
Space group	$P6_5$
Resolution (Å)	50–2.65 (2.70–2.65)
Unit-cell parameters (Å, °)	a = 142.74, b = 142.74, c = 99.80, α = 90, β = 90, γ = 120
$R_{\rm merge}$† (%)	8.1 (42.5)
$\langle I/\sigma(I)\rangle$	24.0 (2.26)
Completeness (%)	95.1 (70.8)
Multiplicity	4.1 (3.5)

† $R_{\rm merge} = \sum_{hkl}\sum_i |I_i(hkl) - \langle I(hkl)\rangle| / \sum_{hkl}\sum_i I_i(hkl)$, where $I_i(hkl)$ is the ith observed intensity of reflection hkl and $\langle I(hkl)\rangle$ is the average intensity over symmetry-equivalent measurements.

2.3. Crystallization

The crystallization screen conditions were from commercial kits (Hampton Research and Emerald BioStructures) together with some home-made products. Initial trials were performed at room temperature using the sitting-drop vapour-diffusion method. The crystallization droplet was comprised of 1.0 µl reservoir solution and 1.0 µl freshly purified full-length or truncated PYL3 mixed with (−)-ABA and was equilibrated against 100 µl reservoir solution. The crystals acquired from the initial trials were further optimized by the hanging-drop vapour-diffusion method. The droplet including 1.0 µl protein–(−)-ABA mixture and 1.0 µl reservoir solution was equilibrated against 500 µl reservoir solution. In order to improve the crystal diffraction resolution, the following measures were adopted: (i) different truncated fragments of PYL3 were used; (ii) the protein concentration in the hanging drop was changed, for example, the volume ratio of protein and reservoir solution was varied over a broad range (1:0.4, 1:0.6, 1:0.8, 1:1, 1:1.2, 1:1.4, 1:1.6, 1:1.8 and 1:2); (iii) the precipitate concentration or buffer pH was changed and (iv) many kinds of additives were used. Gradual dehydration of crystals was carried out to improve the diffraction at the synchrotron-radiation facility. The crystals were soaked step by step in well solutions with 5, 10, 15, 20 and 30% glycerol and were flash-cooled in liquid nitrogen for data collection.

2.4. Data collection and processing

X-ray diffraction data were collected from a single crystal at 100 K on beamline 1W2B at the Beijing Synchrotron Radiation Facility (BSRF) at an X-ray wavelength of 1.0000 Å using a MAR165 CCD detector located at a crystal-to-detector distance of 250 mm. Data for each crystal were collected using an angular range of 360° with an oscillation step of 1.0° and an exposure time of 1 s. All data were integrated and scaled with the *HKL*-2000 suite of programs

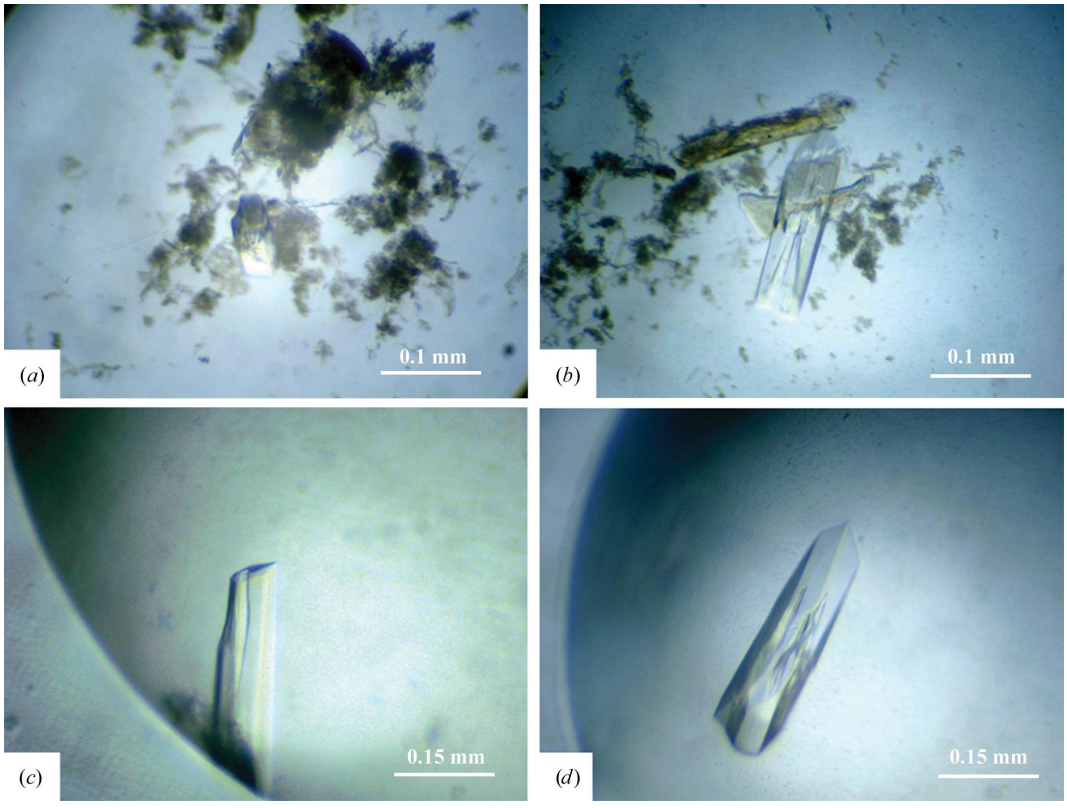

Figure 1
Typical crystals of PYL3–(−)-ABA.

(Otwinowski & Minor, 1997). Data-collection statistics are summarized in Table 1.

3. Results and discussion

Full-length protein and several fragments were concentrated to 20 mg ml^{-1} for crystallization. A PYL3 fragment consisting of residues 21–209 successfully produced single crystals. In the initial screening trials, dozens of small crystals appeared in a 2 µl droplet at 298 K after 3 d. The reservoir solution consisted of 25% PEG 8000, 0.1 *M* Tris–HCl pH 8.0, 0.2 *M* $MgCl_2$. To attenuate crystal nuclei formation, a protein sample supplemented with 5% glycerol was ultracentrifuged at 20 000 rev min^{-1} for 1 h and immediately used in crystallization refinement trials. The concentration of PEG 8000 was also decreased to 20%. After a week of growth without any disturbance, several large crystals of PYL3–(−)-ABA were found in the droplet together with a large amount of protein precipitate (Figs. 1*a* and 1*b*). To avoid an unclear background, the temperature for crystal refinement was changed to 289 K and a few large protein crystals were obtained in a clear droplet. However, this also led to a new problem: rough pits on the surface of the crystal (Figs. 1*c* and 1*d*). This implied crystal-packing imperfections and is consistent with the very low resolution diffraction of many PYL3–(−)-ABA crystals. After extensive efforts testing many hundreds of crystals and step-by-step dehydration using a final concentration of 30% glycerol in the reservoir solution, the best crystal diffracted to 2.65 Å resolution (Fig. 2*a*) and belonged to space group $P6_5$. The corresponding reservoir solution consisted of 20% PEG 8000, 0.1 *M* Tris–HCl pH 8.5, 0.2 *M* $MgCl_2$, 5% glycerol.

To confirm the successful formation of complex crystals, an assay of the inhibition of HAB1 by the PYL3–(−)-ABA crystals was carried out. The inhibitory capacity of the crystals was similar to that of PYL3 with (−)-ABA in solution, thus convincingly revealing the presence of (−)-ABA in the crystals (Supplementary Fig. S2).

The crystals of PYL3–(−)-ABA have an obviously different appearance (Figs. 1*c* and 1*d*) compared with those of apo-PYL3,

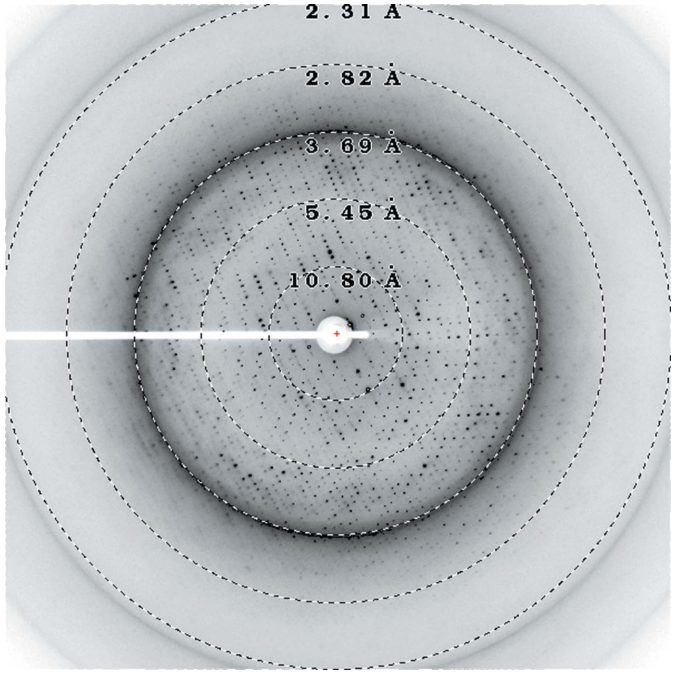

Figure 2
X-ray diffraction image from a PYL3–(−)-ABA crystal.

PYL3–(+)-ABA and PYL3–pyrabacin (Zhang, Wu *et al.*, 2012; Zhang, Zhang *et al.*, 2012). Moreover, (−)-ABA promoted activation of the ABA receptor PYL3, favouring the binding and inhibition of PP2Cs (Supplementary Fig. S3), just like (+)-ABA (Zhang, Zhang *et al.*, 2012). Therefore, (−)-ABA-bound PYL3 may be in a *trans*-dimeric state. Structure determination and *in vitro* biochemical experiments are currently in progress.

We thank Dr Zhongzhou Chen for carefully revising the manuscript. The project was supported by the Starting Research Fund of Guangdong Medical College (XB1341) and is also supported by the National Basic Research Program of China (973 Program; 2011CB965304 and 2009CB825501) and the National Natural Science Foundation of China (31222032, 90919043 and 31070664).

References

Cutler, S. R., Rodriguez, P. L., Finkelstein, R. R. & Abrams, S. R. (2010). *Annu. Rev. Plant Biol.* **61**, 651–679.
Dupeux, F., Santiago, J., Betz, K., Twycross, J., Park, S.-Y., Rodriguez, L., Gonzalez-Guzman, M., Jensen, M. R., Krasnogor, N., Blackledge, M., Holdsworth, M., Cutler, S. R., Rodriguez, P. L. & Márquez, J. A. (2011). *EMBO J.* **30**, 4171–4184.
Fujii, H., Chinnusamy, V., Rodrigues, A., Rubio, S., Antoni, R., Park, S.-Y., Cutler, S. R., Sheen, J., Rodriguez, P. L. & Zhu, J.-K. (2009). *Nature (London)*, **462**, 660–664.
Hao, Q., Yin, P., Li, W., Wang, L., Yan, C., Lin, Z., Wu, J. Z., Wang, J., Yan, S. F. & Yan, N. (2011). *Mol. Cell*, **42**, 662–672.
Hao, Q., Yin, P., Yan, C., Yuan, X., Li, W., Zhang, Z., Liu, L., Wang, J. & Yan, N. (2010). *J. Biol. Chem.* **285**, 28946–28952.
Ma, Y., Szostkiewicz, I., Korte, A., Moes, D., Yang, Y., Christmann, A. & Grill, E. (2009). *Science*, **324**, 1064–1068.
Melcher, K. *et al.* (2009). *Nature (London)*, **462**, 602–608.
Melcher, K., Xu, Y., Ng, L.-M., Zhou, X. E., Soon, F.-F., Chinnusamy, V., Suino-Powell, K. M., Kovach, A., Tham, F. S., Cutler, S. R., Li, J., Yong, E.-L., Zhu, J.-K. & Xu, H. E. (2010). *Nature Struct. Mol. Biol.* **17**, 1102–1108.
Milborrow, B. V. (1974). *Annu. Rev. Plant Physiol.* **25**, 259–307.
Miyazono, K., Miyakawa, T., Sawano, Y., Kubota, K., Kang, H.-J., Asano, A., Miyauchi, Y., Takahashi, M., Zhi, Y., Fujita, Y., Yoshida, T., Kodaira, K. S., Yamaguchi-Shinozaki, K. & Tanokura, M. (2009). *Nature (London)*, **462**, 609–614.
Nambara, E., Suzuki, M., Abrams, S., McCarty, D. R., Kamiya, Y. & McCourt, P. (2002). *Genetics*, **161**, 1247–1255.
Nishimura, N., Hitomi, K., Arvai, A. S., Rambo, R. P., Hitomi, C., Cutler, S. R., Schroeder, J. I. & Getzoff, E. D. (2009). *Science*, **326**, 1373–1379.
Otwinowski, Z. & Minor, W. (1997). *Methods Enzymol.* **276**, 307–326.
Park, S.-Y. *et al.* (2009). *Science*, **324**, 1068–1071.
Peterson, F. C., Burgie, E. S., Park, S.-Y., Jensen, D. R., Weiner, J. J., Bingman, C. A., Chang, C.-E. A., Cutler, S. R., Phillips, G. N. Jr & Volkman, B. F. (2010). *Nature Struct. Mol. Biol.* **17**, 1109–1113.
Raghavendra, A. S., Gonugunta, V. K., Christmann, A. & Grill, E. (2010). *Trends Plant Sci.* **15**, 395–401.
Santiago, J., Dupeux, F., Round, A., Antoni, R., Park, S.-Y., Jamin, M., Cutler, S. R., Rodriguez, P. L. & Márquez, J. A. (2009). *Nature (London)*, **462**, 665–668.
Santiago, J., Rodrigues, A., Saez, A., Rubio, S., Antoni, R., Dupeux, F., Park, S.-Y., Márquez, J. A., Cutler, S. R. & Rodriguez, P. L. (2009). *Plant J.* **60**, 575–588.
Umezawa, T., Nakashima, K., Miyakawa, T., Kuromori, T., Tanokura, M., Shinozaki, K. & Yamaguchi-Shinozaki, K. (2010). *Plant Cell Physiol.* **51**, 1821–1839.
Yin, P., Fan, H., Hao, Q., Yuan, X., Wu, D., Pang, Y., Yan, C., Li, W., Wang, J. & Yan, N. (2009). *Nature Struct. Mol. Biol.* **16**, 1230–1236.
Yuan, X., Yin, P., Hao, Q., Yan, C., Wang, J. & Yan, N. (2010). *J. Biol. Chem.* **285**, 28953–28958.
Zhang, X., Wu, W. & Chen, Z. (2012). *Acta Cryst.* F**68**, 479–482.
Zhang, X., Zhang, Q., Xin, Q., Yu, L., Wang, Z., Wu, W., Jiang, L., Wang, G., Tian, W., Deng, Z., Wang, Y., Liu, Z., Long, J., Gong, Z. & Chen, Z. (2012). *Structure*, **20**, 780–790.